Quantum Electronics **45** (10) 965–972 (2015)

PACS numbers: 42.81.Pa; 07.60.Ly; 07.60.Vg
DOI: 10.1070/QE2015v045n10ABEH015866

Sensitivity of a fibre scattered-light interferometer to external phase perturbations in an optical fibre

A.E. Alekseev, B.G. Gorshkov, V.T. Potapov

Abstract. **Sensitivity of a fibre scattered-light interferometer to external phase perturbations is studied for the first time. An expression is derived for an average power of a useful signal at the interferometer output under external harmonic perturbations in a signal fibre of the interferometer. It is shown that the maximum sensitivity of the scattered-light interferometer depends on the dispersion of the interferogram intensity. An average signal-to-noise ratio is determined theoretically and experimentally at the output of the interferometer at different amplitudes of external perturbations. Using the measured dependences of the signal-to-noise ratio, the threshold sensitivity of the fibre scattered-light interferometer to external phase perturbations is found. The results obtained can be used to optimise characteristics of optical time-domain reflectometers and to design individual phase-sensitive fibre-optic sensors.**

Keywords: *backscattered radiation, fibre scattered-light interferometer, useful signal power, signal-to-noise ratio, threshold sensitivity.*

1. Introduction

Recently, optical time-domain reflectometry has considerably developed thanks to its unique property of locating breaks and dynamic anomalies in lengthy fibre-optic lines [1–5]. However, despite a large number of works devoted to this subject, many parameters of coherent optical time-domain reflectometers (OTDRs) remain poorly understood. A basic object that allows one to study the main properties of a coherent OTDR is a fibre scattered-light interferometer (FSLI), which in the simplest case is a segment of a single-mode optical fibre backscattering coherent laser light. A fibre-optic line of a more complex object – a coherent OTDR – can be represented as a cascade of FSLIs, following one another.

A.E. Alekseev V.A. Kotel'nikov Institute of Radio Engineering and Electronics, Fryazino Branch, Russian Academy of Sciences, pl. Vvedenskogo 1, 114190 Fryazino, Moscow region, Russia; OOO 'Petrofaiber', Klinskii proezd 7, 301664 Novomoskovsk, Tula region, Russia; e-mail: aleksey.e.alekseev@gmail.com;
B.G. Gorshkov OOO 'Petrofaiber', Klinskii proezd 7, 301664 Novomoskovsk, Tula region, Russia; A.M. Prokhorov General Physics Institute, Russian Academy of Sciences, ul. Vavilova 38, 119991 Moscow, Russia;
V.T. Potapov V.A. Kotel'nikov Institute of Radio Engineering and Electronics, Fryazino Branch, Russian Academy of Sciences, pl. Vvedenskogo 1, 114190 Fryazino, Moscow region, Russia; e-mail: v_potapov38@mail.ru

Received 28 May 2015
Kvantovaya Elektronika **45** (10) 965–972 (2015)
Translated by I.A. Ulitkin

A key feature of scattered-light interference is an essentially random nature of the processes occurring during the summation of quasi-monochromatic scattered fields; therefore, scattered-light interferometry and coherent optical time-domain reflectometry can be properly addressed only by using statistical methods. In previous works we examined in detail statistical properties of coherent backscattered light in a single-mode optical fibre [6–8], obtained expressions for the average intensity and backscattered light intensity, as well as for the average spectral characteristics of backscattered light [9]. In this paper we consider the problem of the FSLI response to the external phase perturbations in an optical fibre. The results of this study can serve as a basis for assessing the sensitivity of a coherent phase-sensitive reflectometer [10, 11].

In contrast to the classical Michelson and Mach–Zehnder interference schemes, a FSLI is characterised by multipath interference of random fields of radiations scattered by different scattering centres, i.e. thermodynamic irregularities in the refractive index of optical fibre. We showed in [9] that a FSLI (on average over an ensemble of independent distributions of scattering centres, which we denote by $\{\rho\}$) can be represented as a combination of an infinite number of elementary, independent Michelson interferometers in which scattering centres act as reflecting mirrors. As any interferometer, a FSLI responds to external perturbations and therefore can be used as a sensor of external actions in an optical fibre. An external perturbation, provided that it does not lead to the loss of the radiation power, causes phase modulation of optical radiation propagating in the FSLI. The FSLI response to external perturbations, i.e. the change in intensity of scattered light at its output during the action on a sensitive fibre, depends both on the position of the operating points of all the elementary Michelson interferometers formed by scattering centres and on the scattering amplitudes of these centres. By virtue of the fact that under the influence of the ambient medium the field amplitudes and phases of scattered radiation vary randomly, the interferometer response also varies randomly.

Changes in the scattered light intensity at the output of a FSLI under an external perturbation, which we will also call a useful signal, can be characterised by its power varying with the change in the realisation of the distribution of the coefficients of scattering centres $\{\rho\}$ in fibre. For practical purposes, of interest is the average value of this power, i.e. the useful signal power averaged over $\{\rho\}$. In this paper we consider a simple but important case of an external harmonic perturbation in optical fibre.

The value of the useful signal at the FSLI output and the ensemble-averaged power depend on the interferometer configuration and on the location of the perturbation in the scattering segment. In this paper we consider the scheme of a symmetric two-channel FSLI (an interferometer with two scattering segments of the same length), in which one segment of the fibre is a measuring one, and the second is a reference one. We choose this scheme due to its similarity to the scheme of a coherent OTDR with a double probe pulse [10, 11]. We assume that the main reason for the phase modulation of the radiation under perturbations in a scattering segment of the FSLI is its elongation under the action of an external force, and that the length of the affected region is much smaller than the length of the entire scattering segment, i.e. the external perturbation is point-like.

By simulating a scattering medium, we assume that the complex amplitude coefficient of scattering centres ρ is a circular complex Gaussian random variable with zero mean [6, 7, 12–14], i.e., its real (Reρ) and imaginary (Imρ) parts have a Gaussian distribution over the ensemble, the dispersion of the real and imaginary parts being equal. Physically, this assumption is equivalent to the fact that during scattering the complex amplitude of the field source is multiplied by the random variables with Gaussian distributions of the real and imaginary parts with zero mean. We also assume that the complex amplitude scattering coefficients of different scattering centres are statistically uncorrelated with each other. Mathematically the lack of correlation of the complex coefficients of scattering centres with longitudinal coordinates z_m and z_n, as well as equality of dispersions of their real and imaginary parts can be written in the form of two expressions [14]:

$$E_\rho\langle\rho(z_n)\rho(z_m)\rangle = 0, \tag{1}$$

$$E_\rho\langle\rho^*(z_n)\rho(z_m)\rangle = \rho_0\delta(z_n - z_m), \tag{2}$$

where $E_\rho\langle\ldots\rangle$ is the averaging over $\{\rho\}$ (or averaging over an ensemble of independent scattering segments); $\rho_0/2$ is the dispersion over an ensemble of the real and imaginary parts of the scattering coefficients ρ; and $\delta(\ldots)$ is the delta function.

The light source is assumed to be quasi-monochromatic, whose autocorrelation function of the complex field amplitude $A_s(t)$ is [6–8]

$$E_T\langle A_s(t+\tau)A_s^*(t)\rangle = I_s\exp(-|\tau|/\tau_{coh}), \tag{3}$$

where $E_T\langle\ldots\rangle$ is the averaging over time, I_s is the intensity of the light source, and τ_{coh} is the coherence time of the source field.

2. Average power of the useful signal at the two-channel FSLI output under external harmonic phase perturbation

Consider the response of a two-channel FSLI consisting of two scattering segments of equal length L (Fig. 1); additional delays of the fields for radiations propagating in the interferometer and scattered by the first and second segments will be treated equal to each other, i.e., the scheme of a two-channel FSLI is symmetric. Without loss of generality, we assume that the scattered radiation is partially polarised with the degree of polarisation P; the case of total polarisation will be a particular case.

The Hermitian coherence matrix of partially polarised quasi-monochromatic light can be diagonalized by means of a unitary transformation [13]. As a result, in the new basis the partially polarised monochromatic light of intensity $|A|^2$ can be represented as the sum of two uncorrelated radiations polarised orthogonally in the sense of orthogonality of their Jones vectors. The intensities of each of the two orthogonal polarisation components thus have the forms $|A|^2(1-P)/2$ and $|A|^2(1+P)/2$ [13].

Let one of scattering segments of a symmetrical two-channel FSLI at some point O separated from the beginning of the scattering segment by distance l be exposed to a harmonic perturbation with frequency ω and amplitude m of the form

$$\varphi(t) = m\sin(\omega t), \tag{4}$$

which leads to a periodic elongation of the fibre segment of the FSLI in the mentioned small region, perturbation in the second segment being absent. We will call the segment subjected to external perturbations a signal segment and the other a reference one. Consider how the light intensity changes at the output of a two-channel interferometer.

A perturbation leads to a phase modulation of light scattered by the region after point O. Mentally we divide the reference segment of the FSLI into two segments by point O′,

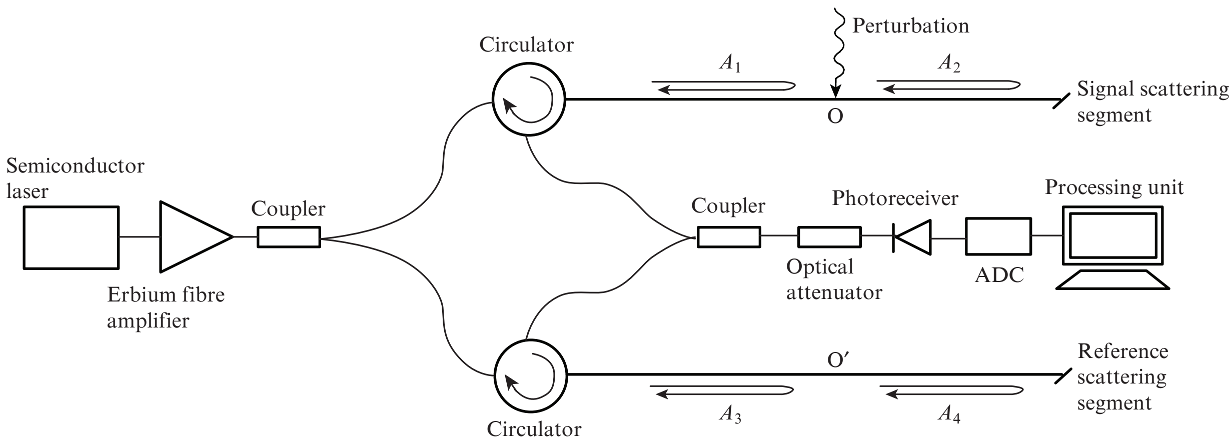

Figure 1. Scheme of the experimental setup of a two-channel FSLI. Here, A_1, A_2, A_3 and A_4 are the complex amplitudes of the fields scattered by the segments [see (5)–(8)].

which is also located at a distance l from its beginning. Assuming that the polarisation states for radiations scattered by the two scattering segments, signal and reference ones, are the same, we will write the complex amplitudes of the light fields for the four fibre segments under consideration in the form [6, 12]

$$[A^{\rho}_{\rm scat}(t)]_1 = \int_0^l A_{\rm s}\Big(t - \frac{2z}{v_{\rm gr}}\Big)\exp(-2{\rm i}kz)\rho_{\rm sig}(z)\,{\rm d}z, \qquad (5)$$

$$[A^{\rho}_{\rm scat}(t)]_2 = \int_l^L A_{\rm s}\Big(t - \frac{2z}{v_{\rm gr}}\Big)\exp[-2{\rm i}kz - 2{\rm i}\eta\varphi(t)]\rho_{\rm sig}(z)\,{\rm d}z, \qquad (6)$$

$$[A^{\rho}_{\rm scat}(t)]_3 = \int_0^l A_{\rm s}\Big(t - \frac{2z}{v_{\rm gr}}\Big)\exp(-2{\rm i}kz)\rho_{\rm ref}(z)\,{\rm d}z, \qquad (7)$$

$$[A^{\rho}_{\rm scat}(t)]_4 = \int_l^L A_{\rm s}\Big(t - \frac{2z}{v_{\rm gr}}\Big)\exp(-2{\rm i}kz)\rho_{\rm ref}(z)\,{\rm d}z, \qquad (8)$$

where k is the constant of light propagation; $v_{\rm gr}$ is the group velocity of light; η is the proportionality factor between the external and phase perturbations in the optical fibre; and subscripts sig and ref indicate that the scattering centre with the longitudinal coordinate z belongs to a signal or to a reference scattering section, and the superscript ρ indicates that the complex amplitudes are written for a fixed realisation of the distribution of the scattering coefficients of centres $\{\rho\}$ of the signal and reference segments. Note also that expressions (5)–(8) are written under the assumption that an identical radiation power is coupled into the signal and reference segments of a two-channel FSLI. Attenuation of the power of radiation propagating along the fibre is neglected because of its smallness at characteristic lengths (100–200 m) of the sections. On writing (6) we have neglected the change in the complex field amplitude of the source, caused by an additional delay that occurs when the fibre is exposed to perturbations.

Because the backscattered radiation is expected to be partially polarised with the degree of polarisation P, the intensity of the respective orthogonally polarised component [13] can be written as

$$[I^{\rho}_{\rm scat}(t)]_{\rm pol1} = \tfrac{1}{2}(1-P)E_T\langle([A^{\rho}_{\rm scat}(t)]_1 + [A^{\rho}_{\rm scat}(t)]_2$$
$$+ [A^{\rho}_{\rm scat}(t)]_3 + [A^{\rho}_{\rm scat}(t)]_4)\times{\rm c.c.}\rangle, \qquad (9)$$

$$[I^{\rho}_{\rm scat}(t)]_{\rm pol2} = \tfrac{1}{2}(1+P)E_T\langle([A^{\rho}_{\rm scat}(t)]_1 + [A^{\rho}_{\rm scat}(t)]_2$$
$$+ [A^{\rho}_{\rm scat}(t)]_3 + [A^{\rho}_{\rm scat}(t)]_4)\times{\rm c.c.}\rangle. \qquad (10)$$

Consider the intensity of totally polarised scattered light, bearing in mind that the intensities of partially polarised light for each of the polarisation components are obtained by multiplying by $(1-P)/2$ and $(1+P)/2$, in accordance with (9) and (10):

$$I^{\rho}_{\rm scat}(t) = E_T\langle([A^{\rho}_{\rm scat}(t)]_1 + [A^{\rho}_{\rm scat}(t)]_2$$
$$+ [A^{\rho}_{\rm scat}(t)]_3 + [A^{\rho}_{\rm scat}(t)]_4)\times{\rm c.c.}\rangle. \qquad (11)$$

After multiplying we obtain 16 terms, ten of which are independent of the external perturbation $\varphi(t)$; they describe the intensity varying with the realisation $\{\rho\}$ in two sections of the interferometer. Six terms with $\varphi(t)$ contain information about the external perturbation. Equation (11) represents a transfer function of a two-channel FSLI; this function determines the response of the interferometer to the external perturbation $\varphi(t)$, corresponding to a fixed realisation $\{\rho\}$ of two sections. The FSLI response changes from one realisation of the distribution of centres $\{\rho\}$ to another in a random manner. Response (11) is nonlinear with respect to an external perturbation $\varphi(t)$; therefore, the signal at the interferometer output will contain frequency harmonics that are absent in the original signal of the external perturbation. A method of demodulation of such a FSLI signal has been considered earlier in [10, 11].

We estimate the power of the useful signal – fluctuations of the scattered light intensity under external perturbations (4) for some fixed realisation of the distribution of the scattering coefficients of centres $\{\rho\}$ of the signal and reference FSLI segments. Terms in (11), containing information about external perturbations, have the form

$$E_T\langle[A^{\rho}_{\rm scat}(t)]_1[A^{\rho}_{\rm scat}(t)]_2^*\rangle = \exp[2{\rm i}\eta\varphi(t)]F^*, \qquad (12)$$

$$E_T\langle[A^{\rho}_{\rm scat}(t)]_1^*[A^{\rho}_{\rm scat}(t)]_2\rangle = \exp[-2{\rm i}\eta\varphi(t)]F, \qquad (13)$$

$$E_T\langle[A^{\rho}_{\rm scat}(t)]_3[A^{\rho}_{\rm scat}(t)]_2^*\rangle = \exp[2{\rm i}\eta\varphi(t)]G^*, \qquad (14)$$

$$E_T\langle[A^{\rho}_{\rm scat}(t)]_3^*[A^{\rho}_{\rm scat}(t)]_2\rangle = \exp[-2{\rm i}\eta\varphi(t)]G, \qquad (15)$$

$$E_T\langle[A^{\rho}_{\rm scat}(t)]_4[A^{\rho}_{\rm scat}(t)]_2^*\rangle = \exp[2{\rm i}\eta\varphi(t)]H^*, \qquad (16)$$

$$E_T\langle[A^{\rho}_{\rm scat}(t)]_4^*[A^{\rho}_{\rm scat}(t)]_2\rangle = \exp[-2{\rm i}\eta\varphi(t)]H. \qquad (17)$$

Here we have introduced the following notations for double integrals:

$$F = E_T\Big\langle\int_0^l\int_l^L A_{\rm s}^*\Big(t-\frac{2z_1}{v_{\rm gr}}\Big)A_{\rm s}\Big(t-\frac{2z_2}{v_{\rm gr}}\Big)$$
$$\times\exp(2{\rm i}kz_1 - 2{\rm i}kz_2)\rho^*_{\rm sig}(z_1)\rho_{\rm sig}(z_2)\,{\rm d}z_1{\rm d}z_2\Big\rangle,$$

$$G = E_T\Big\langle\int_0^l\int_l^L A_{\rm s}^*\Big(t-\frac{2z_1}{v_{\rm gr}}\Big)A_{\rm s}\Big(t-\frac{2z_2}{v_{\rm gr}}\Big)$$
$$\times\exp(2{\rm i}kz_1 - 2{\rm i}kz_2)\rho^*_{\rm ref}(z_1)\rho_{\rm sig}(z_2)\,{\rm d}z_1{\rm d}z_2\Big\rangle,$$

$$H = E_T\Big\langle\int_l^L\int_l^L A_{\rm s}^*\Big(t-\frac{2z_1}{v_{\rm gr}}\Big)A_{\rm s}\Big(t-\frac{2z_2}{v_{\rm gr}}\Big)$$
$$\times\exp(2{\rm i}kz_1 - 2{\rm i}kz_2)\rho^*_{\rm ref}(z_1)\rho_{\rm sig}(z_2)\,{\rm d}z_1{\rm d}z_2\Big\rangle,$$

and have also made an assumption that the external perturbation changes slowly compared to the time fluctuations of the source field. This allows us to remove the corresponding exponential factor from the averaging sign $E_T\langle\ldots\rangle$. Expressions (12) and (13), (14) and (15), and (16) and (17) form complex conjugate pairs. We denote the sum of 10 terms in (11), which do not contain information about the external perturbation, by I_0; then, the transfer function of a two-channel FSLI takes the form

$$I^{\rho}_{\rm scat}(t) = I_0 + \exp[-{\rm i}\varLambda\sin(\omega t)]F + \exp[-{\rm i}\varLambda\sin(\omega t)]G +$$

$$+\exp[-\mathrm{i}\Lambda\sin(\omega t)]H + \exp[\mathrm{i}\Lambda\sin(\omega t)]F^*$$

$$+\exp[\mathrm{i}\Lambda\sin(\omega t)]G^* + \exp[\mathrm{i}\Lambda\sin(\omega t)]H^*, \quad (18)$$

where $\Lambda = 2\eta m$. We will write (18) in the form

$$I^{\rho}_{\rm scat}(t) = I_0 + 2\cos[\Lambda\sin(\omega t)]{\rm Re}X + 2\sin[\Lambda\sin(\omega t)]{\rm Im}X, \quad (19)$$

where we introduce the notation $X = F + G + H$. The useful signal power – temporal intensity fluctuations at the output of a two-channel FSLI – for a fixed realisation of the distribution of scattering coefficients of centres $\{\rho\}$ of two sections corresponds to the dispersion of equation (19); in other words, it is equal to the difference between the total output signal power and the power of a constant component of the signal at the interferometer output:

$$(\sigma_I^{\rho})^2 = E_t\langle I^{\rho}_{\rm scat}(t)I^{\rho}_{\rm scat}(t)\rangle - [E_t\langle I^{\rho}_{\rm scat}(t)\rangle]^2, \quad (20)$$

where $E_t\langle\ldots\rangle$ denotes averaging over time t of the external perturbation. From expression (20) we obtain (see Appendix 1)

$$(\sigma_I^{\rho})^2 = 8({\rm Re}X)^2\sum_{k=1}^{\infty}[J_{2k}(\Lambda)]^2 + 8({\rm Im}X)^2\sum_{k=0}^{\infty}[J_{2k+1}(\Lambda)]^2 \quad (21)$$

or

$$(\sigma_I^{\rho})^2 = 2({\rm Im}X)^2\Lambda^2 \quad (22)$$

for small Λ. We can say that the powers of even components with frequencies $2\omega, 4\omega, \ldots, 2k\omega$ are equal to $8({\rm Re}X)^2[J_{2k}(\Lambda)]^2$, and of odd components with frequencies $\omega, 3\omega, \ldots, (2k+1)\omega$ are equal to $8({\rm Im}X)^2[J_{2k+1}(\Lambda)]^2$. As can be seen, the power of the useful signal at the output of a two-channel FSLI for a specific realisation $\{\rho\}$ depends on the amplitude Λ of the external perturbation as well as on $({\rm Im}X)^2$ and $({\rm Re}X)^2$.

Consider now the average value of the useful signal power (21) over the ensemble of independent distributions of the scattering coefficients of centres $\{\rho\}$ of two sections; we call this value an average power of the useful signal at the output of a two-channel FSLI. To do this, we average expression (21) over the ensemble $\{\rho\}$:

$$\overline{\sigma_I^2} = E_{\rho}\langle(\sigma_I^{\rho})^2\rangle = E_{\rho}\langle 8({\rm Re}X)^2\rangle\sum_{k=1}^{\infty}[J_{2k}(\Lambda)]^2$$

$$+E_{\rho}\langle 8({\rm Im}X)^2\rangle\sum_{k=0}^{\infty}[J_{2k+1}(\Lambda)]^2. \quad (23)$$

The expressions for $E_{\rho}\langle({\rm Re}X)^2\rangle$ and $E_{\rho}\langle({\rm Im}\,X)^2\rangle$ are calculated in Appendix 2. As a result, the expression for the useful signal power averaged over the ensemble $\{\rho\}$ at the output of a two-channel FSLI with two identical scattering segments of length L in the case of exposure of one of the segments to a harmonic phase perturbation with amplitude Λ at point O located at a distance l from the beginning of the scattering segment is given by

$$\overline{\sigma_I^2} = \frac{4(I^{\rm mean}_{\rm scat})^2}{T^2}$$

$$\times\left\{\frac{\tau_{\rm coh}^2}{2}\left[\exp\left(-\frac{2T}{\tau_{\rm coh}}\right) - \exp\left(-\frac{2\theta}{\tau_{\rm coh}}\right)\right] + \tau_{\rm coh}(T-\theta)\right\}\times$$

$$\times\left[\sum_{k=0}^{\infty}[J_{2k+1}(\Lambda)]^2 + \sum_{k=1}^{\infty}[J_{2k}(\Lambda)]^2\right], \quad (24)$$

where $I^{\rm mean}_{\rm scat} = I_{\rm s}(v_{\rm gr}/2)\rho_0 T$ is the scattered light intensity averaged over the ensemble $\{\rho\}$ for one scattering segment [9]; $\theta = 2l/v_{\rm gr}$; and $T = 2L/v_{\rm gr}$.

At small Λ the average power of the useful signal takes the form

$$\overline{\sigma_I^2} = \Lambda^2\frac{(I^{\rm mean}_{\rm scat})^2}{T^2}$$

$$\times\left\{\frac{\tau_{\rm coh}^2}{2}\left[\exp\left(-\frac{2T}{\tau_{\rm coh}}\right) - \exp\left(-\frac{2\theta}{\tau_{\rm coh}}\right)\right] + \tau_{\rm coh}(T-\theta)\right\}. \quad (25)$$

Consider the case of partially polarised scattered light with the polarisation state that is the same for two scattering segments. In this case, the intensity of each of the orthogonal polarisation components is found by multiplying the intensity of totally polarised light by $(1-P)/2$ and $(1+P)/2$, according to (9) and (10). Consequently, the average useful signal powers contained in orthogonal polarisation components can be expressed in terms of the average useful signal powers of totally polarised scattered light (24) or (25):

$$[\overline{\sigma_I^2}]_{\rm pol1} = \tfrac{1}{4}(1-P)^2\overline{\sigma_I^2},$$
$$[\overline{\sigma_I^2}]_{\rm pol2} = \tfrac{1}{4}(1+P)^2\overline{\sigma_I^2}. \quad (26)$$

The total useful signal power averaged over the ensemble $\{\rho\}$ for partially polarised scattered light in the case of exposure of the signal segment of a two-channel FSLI to an external harmonic perturbation is the sum of the average powers of two polarisation components because they are uncorrelated:

$$[\overline{\sigma_I^2}]_{\rm partpol} = \tfrac{1}{2}(1+P^2)\overline{\sigma_I^2}. \quad (27)$$

Thus, the average useful signal power at the output of a two-channel FSLI for partially polarised light is less than for totally polarised radiation by $(1+P^2)/2$ times.

Figure 2 shows the dependences of the average useful signal power with a small external perturbation (25) at the output of a two-channel FSLI, normalised by the square of the

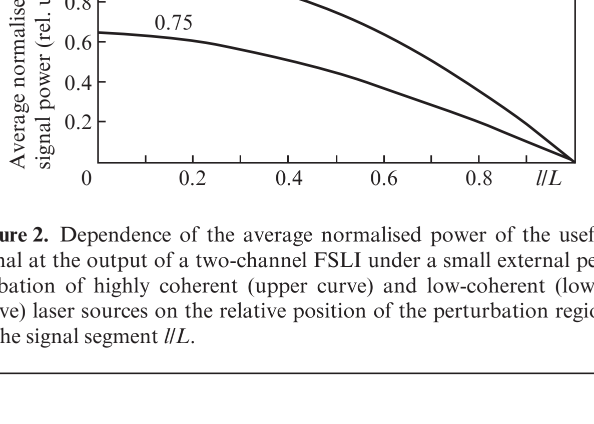

Figure 2. Dependence of the average normalised power of the useful signal at the output of a two-channel FSLI under a small external perturbation of highly coherent (upper curve) and low-coherent (lower curve) laser sources on the relative position of the perturbation region in the signal segment l/L.

mean intensity of the output of a two-channel FSLI, $\overline{\sigma_I^2}/[\Lambda^2(2I_{\rm scat}^{\rm mean})^2]$, on the position of the point of the external perturbation along the signal fibre for two values of $T/\tau_{\rm coh}$.

3. Relation of the average useful signal power at the FSLI output with the dispersion of the scattered light intensity over an ensemble of independent scattering segments

Consider how the normalised useful signal power averaged over the ensemble $\{\rho\}$ at the output of a two-channel FSLI is related to the dispersion of the scattered light intensity over the ensemble $\{\rho\}$, which determines the contrast of a FSLI interferogram or the contrast of a coherent OTDR reflectogram [7, 8]. The dispersion of the intensity of totally polarised backscattered light for a scattering FSLI segment of length L has been found in our previous work [8]:

$$D(I_{\rm scat}) = \frac{(I_{\rm scat}^{\rm mean})^2}{T^2}\left[\frac{\tau_{\rm coh}^2}{2}\exp\left(-\frac{2T}{\tau_{\rm coh}}\right) - \frac{\tau_{\rm coh}^2}{2} + T\tau_{\rm coh}\right]. \quad (28)$$

The dispersion of partially polarised scattered light has the form

$$[D(I_{\rm scat})]_{\rm partpol} = \tfrac{1}{2}(1 + P^2)D(I_{\rm scat}). \quad (29)$$

Figure 3 shows the experimental interferogram at the output of a two-channel FSLI. One can see that the maximum useful signal power averaged over the ensemble $\{\rho\}$ is reached under perturbation at the beginning of the signal scattering segment, i.e. at $l = 0$, or at $\theta = 0$; then, from (25) for totally polarised scattered light we obtain

$$[\overline{\sigma_I^2}]^{\rm max} = \Lambda^2\frac{(I_{\rm scat}^{\rm mean})^2}{T^2}\left[\frac{\tau_{\rm coh}^2}{2}\exp\left(-\frac{2T}{\tau_{\rm coh}}\right) - \frac{\tau_{\rm coh}^2}{2} + T\tau_{\rm coh}\right], \quad (30)$$

which coincides with (28) up to a factor that determines the amplitude of the external perturbation Λ^2. Thus, we have obtained an important result: a maximal normalised average power of the useful signal at the output of a two-channel FSLI is reached, when it is exposed to an external harmonic signal at the beginning of the signal scattering section and is equal to the dispersion of the scattered light intensity of a single scattering segment. Therefore, the dispersion of the backscattered light intensity limits from above the sensitivity of a two-channel FSLI to external phase perturbations.

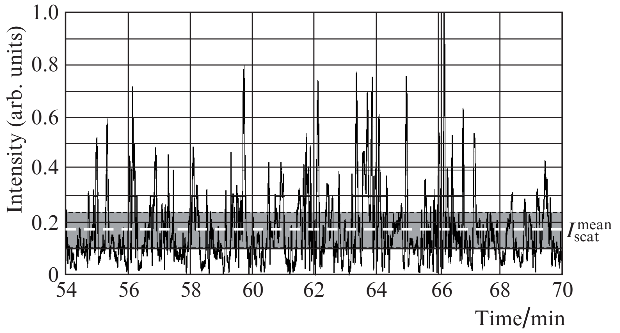

Figure 3. Experimental FSLI interferogram. The white dotted line shows the mean intensity $I_{\rm scat}^{\rm mean}$, the gray area is the standard dispersion of the intensity [the square root of variance (28)].

4. Experimental measurement of the average signal-to-noise ratio at the output of a two-channel FSLI

We will use the results obtained for the average useful signal power at the output of a FSLI exposed to external harmonic perturbations, as well as for the average level of the noise power at the FSLI output found in [9] to estimate the average signal-to-noise ratio (SNR) and the threshold sensitivity of a two-channel FSLI. We have shown in [9] that the noise level at the output of a two-channel FSLI near zero frequency is mainly determined by phase fluctuations of the light source. This circumstance is due to the fact that a FSLI, unlike a Mach–Zehnder and Michelson interferometer, cannot be balanced (between its interfering fields of scattered light there is always a phase delay). The noise power spectral density (NPSD) of the intensity at the FSLI output has a rather cumbersome expression (see [9]); however, in the frequency range close to zero (less than 200 kHz), the NPSD of a FSLI is weakly frequency dependent and therefore can be approximated by a constant (independent of frequency) of the form [9]

$$S_I(f) = \frac{2(I_{\rm scat}^{\rm mean})^2}{T^2}\tau_{\rm coh}\times$$
$$\times\left[\frac{T^2}{2} + \frac{3\tau_{\rm coh}^2}{4} - T\tau_{\rm coh} - \exp\left(-\frac{2T}{\tau_{\rm coh}}\right)\left(\frac{3\tau_{\rm coh}^2}{4} + \frac{T\tau_{\rm coh}}{2}\right)\right]. \quad (31)$$

Expression (31) is valid for totally polarised scattered light with the same polarisation states at the output of the signal and reference scattering FSLI segments. It can be shown that in case of partially polarised scattered light and under the assumption of coincidence of the polarisation state and degree at the outputs of the signal and reference scattering segments, the factor $(1 + P^2)/2$ will appear in (31).

Estimates of the mean-square value of different components of noise currents – shot, thermal and coherent – in the range $\Delta f = 50$ kHz show that the predominant contribution to the noise at the FSLI output (with an excess by 30 dB) is made by the coherent noise caused by phase fluctuations of radiation of a semiconductor laser. Thus, in assessing the average SNR and the threshold sensitivity of the FSLI we should properly take into account only this kind of noise with an average power spectral density near zero frequency (31). We also note that in measurements we should also take into account the flicker noise of the laser and the experimental setup.

The scheme of the experimental setup corresponded to that shown in Fig. 1, the length of the scattering and reference sections being $L = 47.5$ m. The external phase perturbation was provided by a piezoceramic cylinder, onto which a fibre having the length of about 1 m was wound, $l/L = 1/4$. The piezoelectric cylinder with the wound fibre had previously been calibrated to establish a precise correspondence between the amplitude of the voltage applied to it and the amplitude of the resulting phase perturbation. The harmonic signal applied to piezoceramic cylinder had a frequency of 5 kHz. The spectral measurement bandwidth of the FSLI response was $\Delta f = 50$ kHz and was limited by a low-pass filter. We used two types of laser sources with a wavelength in the region of

1555 nm: a laser with a high degree of coherence and with a spectral bandwidth $\Delta\nu$ = 2 kHz, and a laser with a short coherence length and $\Delta\nu$ = 570 kHz.

To determine the average SNR at a fixed amplitude of the external harmonic phase perturbation in fibre, we digitised and measured for 30 s the signal from the photodetector that was installed at the output of a FSLI whose signal arm was exposed to an external modulating signal. Then, using the fast Fourier transform we constructed a periodogram using the Hann window [15]. A typical view of the periodogram, corresponding to an estimate of the average power spectral density of the output interferometer signal for a laser with a high degree of coherence is shown in Fig. 4. The averaged spectrum of the output FSLI signal exhibits spectral harmonics having frequencies that are multiples of the frequency at which the fibre is externally perturbed. The appearance of additional harmonics is associated with the nonlinear response of the FSLI, as follows from (24). One can see from Fig. 4 that the flicker noise increases the total noise level at the interferometer output, its level being above the noise level given by theoretical calculations (31).

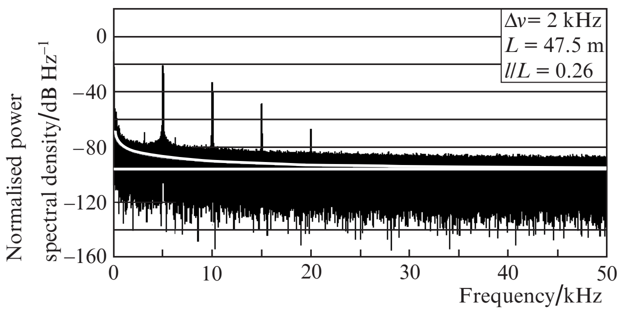

Figure 4. Periodogram of the signal at the output of a two-channel FSLI for estimating the average power spectral density of the signal. The vertical black lines correspond to the harmonics of the useful signal. The horizontal white line is the level of noise caused by phase fluctuations of the laser [see (31)]. The descending white curve shows the flicker noise level of the laser and of the experimental setup.

Thus, using the experimental spectral characteristics we obtained two different estimates of the average SNR:

(i) assuming that the flicker noise is absent, the noise level is taken to be its average level shown in Fig. 4 by a horizontal white line and related to the phase fluctuations of a semiconductor laser; and

(ii) taking into account the total noise power (including the flicker noise of the laser and receiver), the noise level is taken to be its level shown in Fig. 4 by a descending white curve.

The average level of the useful signal power in the detected radiation was estimated by the periodogram, using powers contained in the first harmonics. Figure 5 shows the results of experimental measurements of average SNRs for a two-channel FSLI with a laser of high and low degree of coherence. The frequency f of the external phase perturbation in the signal segment was 5 kHz, the amplitude of the external harmonic phase perturbation Λ varied from 0.0122 to 0.49 rad, and the spectral measurement bandwidth Δf was 50 kHz. We measured both the average SNR without the flicker noise of the laser and the receiver and the average SNR with all the noise in the spectral band Δf = 50 kHz.

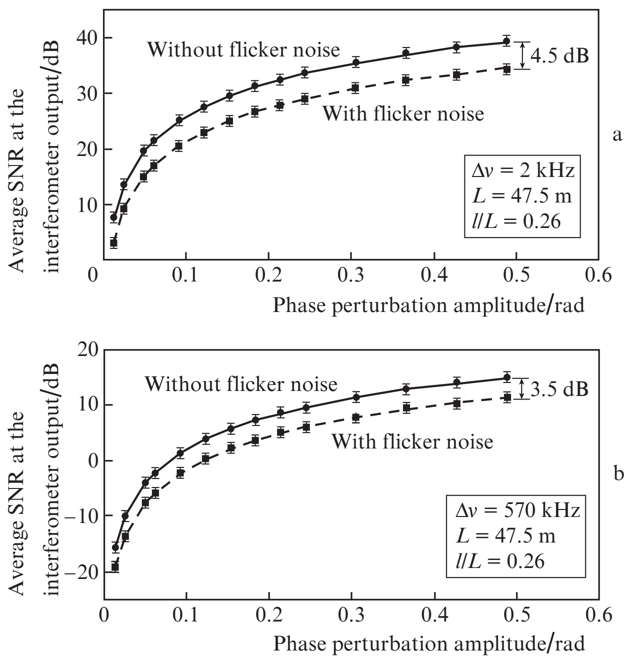

Figure 5. Calculated (curves) and experimental (points) dependences of the average SNR of a two-channel FSLI on the amplitude of the external phase perturbation from a laser with a (a) high and (b) low degree of coherence.

Solid curves in Fig. 5 show the theoretical values of the average SNR with allowance for the noise associated with phase fluctuations of the laser source; the power spectral density is determined by (31) and the power level of the useful signal – by (24) or (25). Dashed curves in Fig. 5 correspond to the theoretical curves shifted down the y axis by an empirical correction factor equal to 4.5 dB for a laser with a high degree of coherence and 3.5 dB for a laser with a low degree of coherence. Thus, taking into account the flicker noise reduces the average SNR compared with the theoretical one by 4.5 dB for a highly coherent laser and by 3.5 dB for a low coherence laser, respectively. One can see from Fig. 5 that the calculations agree with the experiment within the error of ±1 dB for both lasers. In this paper we do not attempt to explain the causes for flicker noise appearance at low frequencies at the FSLI output.

The degree of the scattered light polarisation under the assumption that it is identical for the signal and reference arms of the FSLI does not affect the final value of the average SNR at the output, because for partially polarised scattered light the expressions for the average useful signal power (27) and for NPSD (31) contain a factor $(1 + P^2)/2$, which is reduced by dividing. Similarly, the difference in the polarisation states of light scattered by the two FSLI arms has no effect on the final value of the average SNR, since the expressions for the average useful signal power and for the average NPSD contain the same scalar product of the polarisation vectors of the interfering scattered fields.

Using the data of Fig. 5, we can estimate the threshold sensitivity and minimum detectable signal for a two-channel FSLI with two types of sources. We assume that the signal can be separated from the noise at an average SNR equal to 3 dB in the measurement bandwidth Δf = 50 kHz, and the noise power will be calculated taking into account all the noises in this spectral band. For a laser with $\Delta\nu$ = 2 kHz the minimum experimentally detected phase amplitude of harmonic perturbation is $\Lambda_{\min} = 0.012$ rad, which corresponds to the amplitude of the absolute elongation of the fibre section of 2.6 nm (the theoretical value of the elongation amplitude is 1.52 nm). For a laser with $\Delta\nu = 570$ kHz, $\Lambda_{\min} = 0.17$ rad, which corresponds to the amplitude of the absolute elongation of the fibre segment of 36 nm (the theoretical value of the elongation amplitude is 24 nm).

Thus, flicker noises reduce the FSLI sensitivity and increase the minimum detectable signal for a highly coherent laser by about 70% and for a low coherent laser by about 50%. Note that in this experiment the region of external perturbation has been shifted from the beginning of the signal scattering segment by a quarter of its length; if the point of the perturbation is located closer to the beginning of this section, the useful signal power level will increase (see Fig. 2) and the FSLI will have a better sensitivity threshold.

5. Conclusions

Thus, the issue of the fibre scattered-light interferometer sensitivity to external phase perturbations has been addressed the first time. A notion of the average useful signal power of a FSLI has been introduced. We have obtained expressions for the average useful signal power at the output of a two-channel FSLI exposed to an external point harmonic perturbation in its sensitive fibre. It has been shown that the largest mean value of the useful signal power is reached when the point of perturbation is located at the beginning of the signal segment. We have found that the maximum average power of the useful signal at the FSLI output is determined by the dispersion of the intensity of backscattered light which corresponds to the contrast of the FSLI interferogram. Using the results of previous studies we have determined theoretically and experimentally the average SNR at the output of a two-channel FSLI at different amplitudes of external phase perturbations; theoretical data are in good agreement with the experimental ones if the flicker noise in the setup is taken into account. Using the experimental dependences of the average SNR at the FSLI output we have determined for the first time the two-channel FSLI threshold sensitivity and minimum detectable signal. The studies performed and the results obtained can be applied to assess the sensitivity of coherent OTDRs and fabricate FSLI-based phase-sensitive sensors.

Appendix 1

Consider expression (20) with (19) taken into account:

$$(\sigma_I^\rho)^2 = I_0^2 + 4I_0E_t\langle[\mathrm{Re}X\cos(\Lambda\sin(\omega t))$$
$$+ \mathrm{Im}X\sin(\Lambda\sin(\omega t))]\rangle$$
$$+ 4E_t\langle[\mathrm{Re}X\cos(\Lambda\sin(\omega t)) + \mathrm{Im}X\sin(\Lambda\sin(\omega t))]^2\rangle$$
$$- \{I_0 + 2E_t\langle[\mathrm{Re}X\cos(\Lambda\sin(\omega t)) + \mathrm{Im}X\sin(\Lambda\sin(\omega t))]\rangle\}^2$$
$$= 4E_t\langle[\mathrm{Re}X\cos(\Lambda\sin(\omega t)) + \mathrm{Im}X\sin(\Lambda\sin(\omega t))]^2\rangle$$
$$- 4\{E_t\langle[\mathrm{Re}X\cos(\Lambda\sin(\omega t)) + \mathrm{Im}X\sin(\Lambda\sin(\omega t))]\rangle\}^2$$
$$= 4(\mathrm{Re}X)^2\{E_t\langle\cos^2(\Lambda\sin(\omega t))\rangle - [E_t\langle\cos(\Lambda\sin(\omega t))\rangle]^2\} +$$
$$+ 4(\mathrm{Im}X)^2\{E_t\langle\sin^2(\Lambda\sin(\omega t))\rangle - [E_t\langle\sin(\Lambda\sin(\omega t))\rangle]^2\}.$$

Using the expansion of the sine and cosine in a series of Bessel functions

$$\cos(z\sin\theta) = J_0(z) + 2\sum_{k=1}^{\infty} J_{2k}(z)\cos(2k\theta),$$

$$\sin(z\sin\theta) = 2\sum_{k=0}^{\infty} J_{2k+1}(z)\sin[(2k+1)\theta],$$

we finally obtain (21).

Appendix 2

Let us calculate the average values of $E_\rho\langle(\mathrm{Re}X)^2\rangle$ and $E_\rho\langle(\mathrm{Im}X)^2\rangle$, where $X = F + G + H$. Note that $(\mathrm{Im}X)^2 = -(X - X^*)^2/4$, $(\mathrm{Re}X)^2 = (X + X^*)^2/4$. Thus, we consider the average values of $E_\rho\langle XX^*\rangle$, $E_\rho\langle XX\rangle$ and $E_\rho\langle X^*X^*\rangle$. We expand the product:

$$E_\rho\langle XX\rangle = E_\rho\langle F^2 + G^2 + H^2 + 2FG + 2GH + 2FH\rangle,$$

$$E_\rho\langle X^*X^*\rangle = E_\rho\langle F^{*2} + G^{*2} + H^{*2} + 2F^*G^* + 2G^*H^* + 2F^*H^*\rangle,$$

$$E_\rho\langle XX^*\rangle = E_\rho\langle FF^* + GF^* + HF^* + FG^* + GG^* + HG^*$$
$$+ FH^* + GH^* + HH^*\rangle.$$

We use the Gaussian moment theorem for random complex quantities that are, by assumption, represented by complex scattering coefficients [16]:

$$E_\rho\langle\,\rho_{i1}^*\rho_{i2}^*\ldots\rho_{iN}^*\rho_{j1}\rho_{j2}\ldots\rho_{jM}\,\rangle$$

$$= \begin{cases} 0, N \neq M, \\ \sum\limits_{i,j=1}^{N,M} E_\rho\langle\,\rho_{i1}^*\rho_{j1}\rangle E_\rho\langle\,\rho_{i2}^*\rho_{j2}\rangle\ldots E_\rho\langle\,\rho_{iN}^*\rho_{jM}\rangle,\ N = M. \end{cases}$$

With allowance for (1) and (2) we obtain

$$E_\rho\langle\rho^*(z_1)\rho(z_2)\rho^*(z_3)\,\rho(z_4)\rangle = E_\rho\langle\rho^*(z_1)\rho(z_2)\rangle$$

$$\times E_\rho\langle\rho^*(z_3)\rho(z_4)\rangle + E_\rho\langle\rho(z_2)\rho^*(z_3)\,\rangle E_\rho\langle\rho^*(z_1)\rho(z_4)\rangle$$

$$= \rho_0^2\delta(z_1 - z_2)\delta(z_3 - z_4) + \rho_0^2\delta(z_2 - z_3)\delta(z_1 - z_4). \qquad \text{(A2.1)}$$

In view of (A2.1) and uncorrelated complex scattering amplitudes ρ for centres, which are located on different (before and after the perturbation point O) portions of the signal segment and on different portions of the reference segment separated by a symmetrical point O′, we have the expressions

$$E_\rho\langle FF\rangle = E_\rho\langle F^*F^*\rangle = 0,\quad E_\rho\langle GG\rangle = E_\rho\langle G^*G^*\rangle = 0,$$

$$E_\rho\langle HH\rangle = E_\rho\langle H^*H^*\rangle = 0,\quad E_\rho\langle FG\rangle = E_\rho\langle F^*G^*\rangle = 0,$$

$$E_\rho\langle GH\rangle = E_\rho\langle G^*H^*\rangle = 0,\quad E_\rho\langle FH\rangle = E_\rho\langle F^*H^*\rangle = 0.$$

Therefore, $E_\rho\langle XX\rangle = E_\rho\langle X^*X^*\rangle = 0$, which implies that

$$E_\rho\langle(\mathrm{Re}X)^2\rangle = E_\rho\langle(\mathrm{Im}X)^2\rangle = \frac{1}{2}E_\rho\langle XX^*\rangle. \quad \text{(A2.2)}$$

Similarly, for the terms in the expression for $E_\rho\langle XX^*\rangle$, we have

$$E_\rho\langle FF^*\rangle = \rho_0^2\int_0^l\int_l^L E_T\left\langle A_\mathrm{s}^*\left(t-\frac{2z_1}{v_\mathrm{gr}}\right)A_\mathrm{s}\left(t-\frac{2z_2}{v_\mathrm{gr}}\right)\right\rangle$$

$$\times E_T\left\langle A_\mathrm{s}\left(t-\frac{2z_1}{v_\mathrm{gr}}\right)A_\mathrm{s}^*\left(t-\frac{2z_2}{v_\mathrm{gr}}\right)\right\rangle \mathrm{d}z_1\mathrm{d}z_2,$$

$$E_\rho\langle GG^*\rangle = \rho_0^2\int_0^l\int_l^L E_T\left\langle A_\mathrm{s}^*\left(t-\frac{2z_1}{v_\mathrm{gr}}\right)A_\mathrm{s}\left(t-\frac{2z_2}{v_\mathrm{gr}}\right)\right\rangle$$

$$\times E_T\left\langle A_\mathrm{s}\left(t-\frac{2z_1}{v_\mathrm{gr}}\right)A_\mathrm{s}^*\left(t-\frac{2z_2}{v_\mathrm{gr}}\right)\right\rangle \mathrm{d}z_1\mathrm{d}z_2,$$

$$E_\rho\langle HH^*\rangle = \rho_0^2\int_l^L\int_l^L E_T\left\langle A_\mathrm{s}^*\left(t-\frac{2z_1}{v_\mathrm{gr}}\right)A_\mathrm{s}\left(t-\frac{2z_2}{v_\mathrm{gr}}\right)\right\rangle\times$$

$$\times E_T\left\langle A_\mathrm{s}\left(t-\frac{2z_1}{v_\mathrm{gr}}\right)A_\mathrm{s}^*\left(t-\frac{2z_2}{v_\mathrm{gr}}\right)\right\rangle \mathrm{d}z_1\mathrm{d}z_2,$$

$$E_\rho\langle GF^*\rangle = 0,\ E_\rho\langle HF^*\rangle = 0,\ E_\rho\langle FG^*\rangle = 0,$$

$$E_\rho\langle HG^*\rangle = 0,\ E_\rho\langle FH^*\rangle = 0,\ E_\rho\langle GH^*\rangle = 0.$$

Hence, $E_\rho\langle XX^*\rangle = E_\rho\langle FF^*\rangle + E_\rho\langle GG^*\rangle + E_\rho\langle HH^*\rangle$. Using (A2.1) and making the change of variables $\tau_1 = 2z_1/v_\mathrm{gr}$, $\tau_2 = 2z_2/v_\mathrm{gr}$, we obtain

$$E_\rho\langle XX^*\rangle = \frac{v_\mathrm{gr}^2}{4}\rho_0^2 I_\mathrm{s}^2\int_0^\theta\int_\theta^T \exp\left(-\frac{2|\tau_2-\tau_1|}{\tau_\mathrm{coh}}\right)\mathrm{d}\tau_1\mathrm{d}\tau_2$$

$$+\frac{v_\mathrm{gr}^2}{4}\rho_0^2 I_\mathrm{s}^2\int_0^\theta\int_\theta^T \exp\left(-\frac{2|\tau_2-\tau_1|}{\tau_\mathrm{coh}}\right)\mathrm{d}\tau_1\mathrm{d}\tau_2$$

$$+\frac{v_\mathrm{gr}^2}{4}\rho_0^2 I_\mathrm{s}^2\int_\theta^T\int_\theta^T \exp\left(-\frac{2|\tau_2-\tau_1|}{\tau_\mathrm{coh}}\right)\mathrm{d}\tau_1\mathrm{d}\tau_2. \quad \text{(A2.3)}$$

Hence, after the evaluation of the integrals we obtain

$$E_\rho\langle XX^*\rangle = \frac{v_\mathrm{gr}^2}{4}\rho_0^2 I_\mathrm{s}^2$$

$$\times\left\{\frac{\tau_\mathrm{coh}^2}{2}\left[\exp\left(-\frac{2T}{\tau_\mathrm{coh}}\right)-\exp\left(-\frac{2\theta}{\tau_\mathrm{coh}}\right)\right]+\tau_\mathrm{coh}(T-\theta)\right\}. \quad \text{(A2.4)}$$

The sought-for expressions $E_\rho\langle(\mathrm{Re}X)^2\rangle$ and $E_\rho\langle(\mathrm{Im}X)^2\rangle$ are related to (A2.4) through (A2.2).

References

1. Shatalin S.V., Treschikov V.N., Rogers A.J. *Appl. Opt*., **37** (24), 5600 (1998).
2. Juarez J.C., Maier E.W., Kyoo Nam Choi, Taylor H.F. *J. Lightwave Technol*., **23** (6), 2081 (2005).
3. Gorshkov B.G., Paramonov V.M., Kurkov A.S., Kulakov A.T., Zazirnyi M.V. *Kvantovaya Elektron*., **36** (10), 963 (2006) [*Quantum Electron*., **36** (10), 963 (2006)].
4. Vdovenko V.S., Gorshkov B.G., Zazirnyi M.V., Kulakov A.T., Kurkov A.S., Paramonov V.M. *Kvantovaya Elektron*., **41** (2), 176 (2011) [*Quantum Electron*., **41** (2), 176 (2011)].
5. Nesterov E.T., Treshchikov V.N., Ozerov A.Zh., Sleptsov M.A., Kamynin V.A., Nanii O.E., Sus'yan A.A. *Pis'ma Zh. Tekh. Fiz*., **37** (9), 55 (2011).
6. Alekseev A.E., Tezadov Ya.A., Potapov V.T. *Radiotekh. Elektron*., **56** (12), 1522 (2011).
7. Alekseev A.E., Tezadov Ya.A., Potapov V.T. *Kvantovaya Elektron*., **42** (1), 76 (2012) [*Quantum Electron*., **42** (1), 76 (2012)].
8. Alekseev A.E., Gorshkov B.G., Potapov V.T. *Kvantovaya Elektron*., **45** (8), 748 (2015) [*Quantum Electron*., **45** (8), 748 (2015)].
9. Alekseev A.E., Potapov V.T. *Kvantovaya Elektron*., **43** (10), 968 (2013) [*Quantum Electron*., **43** (10), 968 (2013)].
10. Alekseev A.E., Vdovenko V.S., Gorshkov B.G., Potapov V.T., Sergachev I.A., Simikin D.E. *Kvantovaya Elektron*., **44** (10), 965 (2014) [*Quantum Electron*., **44** (10), 965 (2014)].
11. Alekseev A.E., Vdovenko V.S., Gorshkov B.G., Potapov V.T., Simikin D.E. *Laser Phys*., **24** (11), 115106 (2014).
12. Gysel P., Staubli R.K. *J. Lightwave Technol*., **8** (4), 561 (1990).
13. Goodman J.W. *Statistical Optics* (New York: Wiley, 1985; Moscow: Mir, 1988).
14. Goodman J.W. In: *Laser Speckle and Related Phenomena*. Ed. by J.C. Dainty (Berlin: Springer-Verlag, 1975).
15. Sergienko A.B. *Tsifrovaya obrabotka signalov* (Digital Signal Processing) (St Petersburg: Piter, 2003).
16. Mandel L., Wolf E. *Optical Coherence and Quantum Optics* (Cambridge: Cambridge University Press, 1995; Moscow: Nauka, 2000).